

Effects of first-order approximations on head and specific discharge covariances in high-contrast log conductivity

Thomas Van Lent

Department of Civil and Environmental Engineering, South Dakota State University, Brookings

Peter K. Kitanidis

Department of Civil Engineering, Stanford University, Stanford, California

Abstract. The hydraulic head and the specific discharge fluctuations depend nonlinearly on the hydraulic conductivity. However, the methods most commonly used in the stochastic analysis of groundwater flow are based upon the linearization of these relations. In this paper we apply a numerical spectral approach to investigate the range of validity of the small perturbation approximation for head and specific discharge moments in two-dimensional finite domains. We find that the small perturbation approximation tends to underestimate the variance of large-scale head and specific discharge fluctuations and error increases with increasing log-conductivity variance and increasing domain size. The head fluctuations do not appear ergodic even when the small perturbation approximation predicts they will be ergodic. The specific discharge fluctuations, on the other hand, do appear ergodic. The small perturbation approximation performs well in estimating specific discharge variance in the longitudinal direction but significantly underestimates transverse specific discharge variance.

Introduction

Groundwater flow and transport problems are characterized by uncertainty; the hydrogeologic parameters of a problem are rarely known with precision. This uncertainty may strongly affect the reliability of predictions made about the aquifer. However, accounting for this uncertainty in a mathematically rigorous way results in unwieldy formulations of the governing equations of groundwater flow and solute transport, as well as a formidable statistical inference problem. To obtain tractable mathematics and develop practical methods, researchers have made simplifications, usually by assuming that the fluctuating components are small in some sense. This work focuses on the applicability of the small perturbation approximation for flow in high-contrast, heterogeneous, random, porous media.

Small perturbation approximations of stochastic groundwater flow and transport problems are approximate solutions to governing differential equations using asymptotic expansions. When those perturbations are small, then the expansion can be truncated after very few terms, usually only one or two. When the expansion is truncated after the first term, it is called a first-order, small perturbation, or linearized solution. There are numerous examples of this type of analysis applied to groundwater flow problems. *Sagar* [1978] developed a stochastic finite element procedure after applying a small perturbation approximation. *Dettinger and Wilson* [1981] proposed a similar method, using only the first-order terms of a Taylor series expansion, claiming that this could be used to ease the computational burden of Monte Carlo simulations. *Dagan* [1982a, b] used perturbation expansions in order to develop relations for effective conductivity and head variograms. *Mizell et al.* [1982] used a linear approximation to investigate the condi-

tions which lead to stationarity of the head fluctuations. *Dikow* [1988] used a Fourier series method combined with small perturbation approximations to compute mass fluxes in groundwater flow. *Li and McLaughlin* [1991, 1995] extend the small perturbation approximation by using a numerical approach to apply boundary conditions in a Fourier domain. The small perturbation approximation underlies much of the linear theory of flow and transport in random porous media; *Dagan* [1989] and *Gelhar* [1993] present thorough introductions to the topic.

One particular analysis technique combining a small perturbation approximation with Fourier analysis has found wide application. *Gelhar* [1977] first applied Fourier analysis to examine stochastic spatial variability. The development of spectral methods in groundwater flow continued with contributions by *Bakr et al.* [1978] and *Mizell et al.* [1982]. Both of these efforts employed the small perturbation approximation on the flow equations to investigate the effects of dimensionality and spatial correlation on head variance. The small perturbation method has also been applied to problems involving solute transport in groundwater, beginning largely with *Gelhar and Axness* [1983]. There, the linearized forms for the advection-dispersion and flow equations were used to examine solute transport in an aquifer with conductivity varying in three dimensions. They derived expressions for the dispersivities (parameters used to scale the dispersion term in the advection-diffusion equation) as functions of the log-conductivity fluctuations. *Dagan* [1987] presented a unified theory of macrodispersion, incorporating *Gelhar and Axness* [1983] and *Newman et al.* [1987] as special cases. *Dagan's* expressions for the moments describing the spreading of a contaminant plume require the Fourier transform of the velocity covariances, which are difficult to obtain analytically. The small perturbation approximation is used as a type of closure approximation for relating moments of random variables related by the gov-

Copyright 1996 by the American Geophysical Union.

Paper number 96WR00196.
0043-1397/96/96WR-00196\$09.00

erning stochastic, partial differential equations of flow and transport.

The range of validity of the closure approximation has received considerable attention. *Dagan* [1985, 1988] indicates the approximation for head second moments is valid for log conductivities up to about unity; many other researchers have commented upon the robustness of the approximation. *Ababou et al.* [1988, 1989] have put forth numerical experimental evidence to support their contention that the small perturbation approximation as applied to the equations of groundwater flow is valid up to log-conductivity variances of at least 4. *Jones* [1989] used a Monte Carlo technique to examine the effects of log-conductivity variances and well pumping rates and tested the validity of first-order approximations of *Dettinger and Wilson* [1981]. He concludes that log-conductivity variances larger than unity can affect the validity of the linearized approximation. *Dagan and Neuman* [1991] offer some evidence that for the stochastic advection-dispersion equation, the neglected terms in the small perturbation methods may be the same order as those retained. Numerical investigations have been undertaken by a number of investigators [e.g., *Smith and Schwartz*, 1980, 1981; *Rubin*, 1990; *Chin and Wang*, 1992; *Bellin et al.*, 1992, 1994]. Of particular interest to this investigation are the results of *Bellin et al.* [1992], who exhaustively examine velocity moments. In this work we confine our examinations to the behavior of the second moments of head and specific discharge and the range of validity of the small perturbation approximation for predicting those moments.

Methods

The numerical method applied in this investigations is the numerical spectral method similar to that used by *Dykaar and Kitanidis* [1992] to compute effective conductivities and by *Fiorotto and Giorgini* [1992] for unsteady groundwater flow. The procedure is based upon an integral transformation of the governing equations and is the numerical analog to the analytical procedures applied by *Gelhar and Axness* [1983] and *Gutjahr et al.* [1978]. The governing equation for groundwater flow in an isotropic porous media with no sources or sinks is taken as

$$\frac{\partial}{\partial x_i} \left[K(\mathbf{x}) \frac{\partial \phi}{\partial x_i} \right] = 0 \quad (1)$$

where $K(\mathbf{x})$ is the hydraulic conductivity, ϕ is the head, and x_i is the coordinate in the i th principal direction ($i = 1, 2, \dots, n$ where n is the dimensionality) and where we have used an Einstein notation to denote the summation over i . The typical analytical approach is to assume that

$$\phi(\mathbf{x}) = -J_i x_i + h(\mathbf{x}) \quad (2a)$$

$$\ln K(\mathbf{x}) = Y(\mathbf{x}) = Y(\mathbf{x}) + f(\mathbf{x}) \quad (2b)$$

where J_i is the mean head gradient in direction i , $h(\mathbf{x})$ is a zero-mean head fluctuation, $Y(\mathbf{x})$ is the mean log conductivity, and $f(\mathbf{x})$ is a zero-mean log-conductivity fluctuation. These fluctuations are taken as stationary, with covariances defined by

$$R_{hh}(\boldsymbol{\xi}) = E[h(\mathbf{x})h(\mathbf{x} + \boldsymbol{\xi})] \quad (3)$$

$$R_{ff}(\boldsymbol{\xi}) = E[f(\mathbf{x})f(\mathbf{x} + \boldsymbol{\xi})] \quad (4)$$

where $\boldsymbol{\xi}$ is a separation vector. In these investigations we take the x_1 direction coincidental with the direction of the mean head gradient and $Y(\mathbf{x})$ as a constant. These assumptions are adopted to facilitate comparison with analytical results. Substitution of (2a)–(2b) into (1) will result in a governing relation between the fluctuating components

$$\frac{\partial^2 h(\mathbf{x})}{\partial x_i^2} + \frac{\partial f(\mathbf{x})}{\partial x_i} \frac{\partial h(\mathbf{x})}{\partial x_i} = J_i \frac{\partial f(\mathbf{x})}{\partial x_i} \quad (5)$$

The choice of boundary conditions will necessarily determine the solution to the above boundary value problem. The typical approach for a numerical scheme is to apply deterministic boundary constant head and no-flux boundary conditions. The constant head boundary condition introduces nonstationarities into the heads [*Smith and Freeze*, 1979a, b; *Rubin and Dagan*, 1988]. The no-flux boundary condition imposes two straight streamlines using a periodic reflection [*Rubin and Dagan*, 1989]. The periodicity assumption employed here is more general and imposes fewer constraints on the flow domain. The entire domain is usable for estimation of head and specific discharge covariances, and one need not specify an inner core thought to be unaffected by boundary effects.

In these investigations we impose boundary conditions such that the head and log-conductivity fields are approximately stationary in a finite domain. Stationarity, in its most general form, is formulated in an infinite domain, since it allows for spatial variability at all scales. However, numerical procedures require finite domains, and stationarity can only be approximated. In the classical development of stationary stochastic processes, infinite domains are obtained by first assuming periodicity and then taking the limit as the period goes to infinity [*Priestley*, 1981, p. 206]. The periodic boundary conditions, assuming that x_i is normalized by some period L_i and the domain is two dimensional, would be

$$h(x_1, \frac{1}{2}) = h(x_1, -\frac{1}{2}) \quad (6a)$$

$$h(\frac{1}{2}, x_2) = h(-\frac{1}{2}, x_2) \quad (6b)$$

$$f(x_1, \frac{1}{2}) = f(x_1, -\frac{1}{2}) \quad (6c)$$

$$f(\frac{1}{2}, x_2) = f(-\frac{1}{2}, x_2) \quad (6d)$$

One can formulate approximations for the head and log-conductivity fluctuations meeting the above boundary conditions as Fourier series

$$f(\mathbf{x}) = \sum_{\text{all } \mathbf{k}} F(\mathbf{k}) \exp(i2\pi k_i x_i) \quad (7)$$

$$h(\mathbf{x}) = \sum_{\text{all } \mathbf{k}} H(\mathbf{k}) \exp(i2\pi k_i x_i) \quad (8)$$

where $i = \sqrt{-1}$, \mathbf{k} is a wave vector composed of integers, and $H(\mathbf{k})$ and $F(\mathbf{k})$ are the complex Fourier coefficients. Substitution of the above into (5) will transform the governing equation to the Fourier domain

$$k^2 H(\mathbf{k}) + k_j H(\mathbf{k}) * k_j F(\mathbf{k}) = \frac{-i}{2\pi} J_j K_j F(\mathbf{k}) \quad \forall \mathbf{k} \quad (9)$$

where $k^2 = k_j k_j$, and the $*$ operator denotes a convolution sum, defined in this case as

$$G_1(\mathbf{k}) * G_2(\mathbf{k}) = \sum_{\mathbf{k}=\mathbf{r}+\mathbf{s}} G_1(\mathbf{r})G_2(\mathbf{s}) \quad (10)$$

The spectral formulation of the governing equation is approximated by truncating the wavenumber domain \mathbf{k} with cutoff wavenumbers. This amounts to limiting the spatial scales of variability that are included in the calculation. Equation (9) then becomes a system of simultaneous, linear, algebraic equations. This procedure is known as a numerical spectral method. *Dykaar and Kitanidis [1992]*, *Fiorotto and Giorgini [1992]*, and *Van Lent [1992]* provide the procedural methods and details.

A Monte Carlo simulation approach begins by generating random realizations of Fourier transform of log-conductivity fluctuations, $F(\mathbf{k})$. Given the spectrum of the log-conductivity fluctuations, $S_{ff}(\mathbf{k})$, it is straightforward to generate realizations of $F(\mathbf{k})$ by [*Gutjahr, 1989*]

$$F(\mathbf{k}) = \sqrt{S_{ff}(\mathbf{k})}e^{i\theta} \quad (11)$$

where θ is a random phase angle, $-\pi \leq \theta \leq \pi$, and $\theta(\mathbf{k}) = \theta(-\mathbf{k})$. *Robin et al. [1993]* demonstrate the advantages of these fast Fourier transform (FFT)-based methods, particularly for reproducing the input covariance. Realizations of $F(\mathbf{k})$ are then used to solve for the Fourier transform of the head fluctuations $H(\mathbf{k})$ using (9). The spectrum of the head is then estimated by

$$\hat{S}_{hh}(\mathbf{k}) = \frac{1}{M} \sum_{l=1}^M H_l^*(\mathbf{k})H_l(\mathbf{k}) \quad (12)$$

where the subscript l refers to the $H(\mathbf{k})$ obtained from the l th realization of $F(\mathbf{k})$ and M is the number of Monte Carlo realizations.

One can calculate the specific discharge in direction j as

$$\begin{aligned} Q_j(\mathbf{x}) &= -K(\mathbf{x}) \frac{\partial \phi}{\partial x_j} \\ Q_j(\mathbf{x}) &= -K_G \exp [f(\mathbf{x})] \left(-J_j + \frac{\partial h}{\partial x_j} \right) \\ Q_j(\mathbf{x}) &= \bar{q}_j + q_j(\mathbf{x}) \end{aligned} \quad (13)$$

where $K_G = e^Y$ and $\bar{q}_j = K_G J_j$. *Van Lent [1992]* provides details on how the specific discharge fluctuation in the j th direction is efficiently calculated with a numerical spectral method. This method involves a discretization of the spectral domain. In discrete form, (9) becomes

$$(K^2 C M_j C^{-1} K_j) H = J_j K_j F \quad (14)$$

where C denotes the fast Fourier transform operator, F is discrete matrix representation of (11), K_j is the wave space matrix defined such that $C^{-1} K_j C(\)$ is equivalent to the physical space operation $\partial(\)/\partial x_j$, and $M_j = \text{diag}(C^{-1} K_j F)$. Equation (14) is a system of simultaneous, linear, algebraic equations and is solved for H , the Fourier transform of the head fluctuations. The specific discharge is then calculated using

$$\mathcal{Q}_j = -K_G C [\exp(C^{-1} F) (-J_j + C^{-1} K_j H)] \quad (15)$$

The calculation procedure is often summarized by saying that differentiation is done as a multiplication in Fourier space and multiplications are done in physical space and transformed

back to Fourier space. The spectrum of \mathcal{Q}_j is then estimated from

$$\hat{S}_{q_{qj}}(\mathbf{k}) = \frac{1}{M} \sum_{l=1}^M \mathcal{Q}_{-il}(\mathbf{k}) \mathcal{Q}_{jl}^*(\mathbf{k}) \quad (16)$$

where \mathcal{Q}_{jl} is the l th realization of the Fourier transform of the q_j component.

An important consideration in any numerical approach is to assure numerical accuracy. *Bellin et al. [1992]* discuss the importance of the convergence properties of a Monte Carlo approach for establishing the accuracy of both the numerical solution and the moment estimate. We found the convergence criterion a particularly important concern when calculating specific discharge variance. Local violations of continuity can lead to errors in the estimate of specific discharge variance and distort the calculations of specific discharge moments. In a numerical spectral approach, errors in the specific discharge fluctuations evidence themselves in both physical and wave spaces. Figure 1a shows how localized oscillations, related to Gibbs phenomena, can occur if discretization is inadequate to resolve all important scales of specific discharge fluctuation. In wave space the errors appear as incongruously high variance at small scales (large wavenumbers), as shown in Figure 1b. These errors are local violations of the requirement of zero divergence of the specific discharge and lead to inaccurate estimates of specific discharge moments.

To guard against these potential violations of continuity, we applied three techniques. First, we smoothed the log-conductivity field by applying a band-pass filter. By limiting small-scale variability in log conductivity the calculations of small-scale specific discharge variability are much less susceptible to error. This smoothing tends to decrease the range of log-conductivity variances which can be examined but is essential for numerical accuracy. The smoothing is done as follows. The domain is discretized into $N \times N$ nodes, giving a maximum resolvable wavenumber of $k_{\max} = N/2$. We found that smoothing done with a simple band-pass filter

$$\begin{aligned} F(\mathbf{k}) &= F(\mathbf{k}) \quad |\mathbf{k}| < K_c \\ F(\mathbf{k}) &= 0 \quad \text{otherwise} \end{aligned} \quad (17)$$

was sufficient. The cutoff wavenumber K_c was taken such that the log-conductivity field was oversampled by a factor of 2–4; that is, K_c was one half to one fourth of k_{\max} . The factor of 2 oversampling was sufficient for small log-conductivity variance problems but needed to be increased as log conductivity increases. In this way, one can accurately calculate the small-scale specific discharge fluctuations without the errors seen in Figure 1.

Figure 2 shows how this filtering leads to slightly different input log-conductivity covariances. In particular, the total variance, $R_{ff}(0)$, gets reduced, because some small-scale variability is being filtered. This also has the effect of smoothing the log conductivity in the sense that the curvature of $R_{ff}(0)$ decreases. When reporting log-conductivity variances, we use the postfiltered log-conductivity covariance function.

The second procedure we implemented to assure numerical accuracy was to finely discretize the domain, particularly when specific discharge vectors were calculated. A grid of 512×512 nodes was the highest resolution which still feasibly allowed a Monte Carlo approach. Resolutions were limited by available

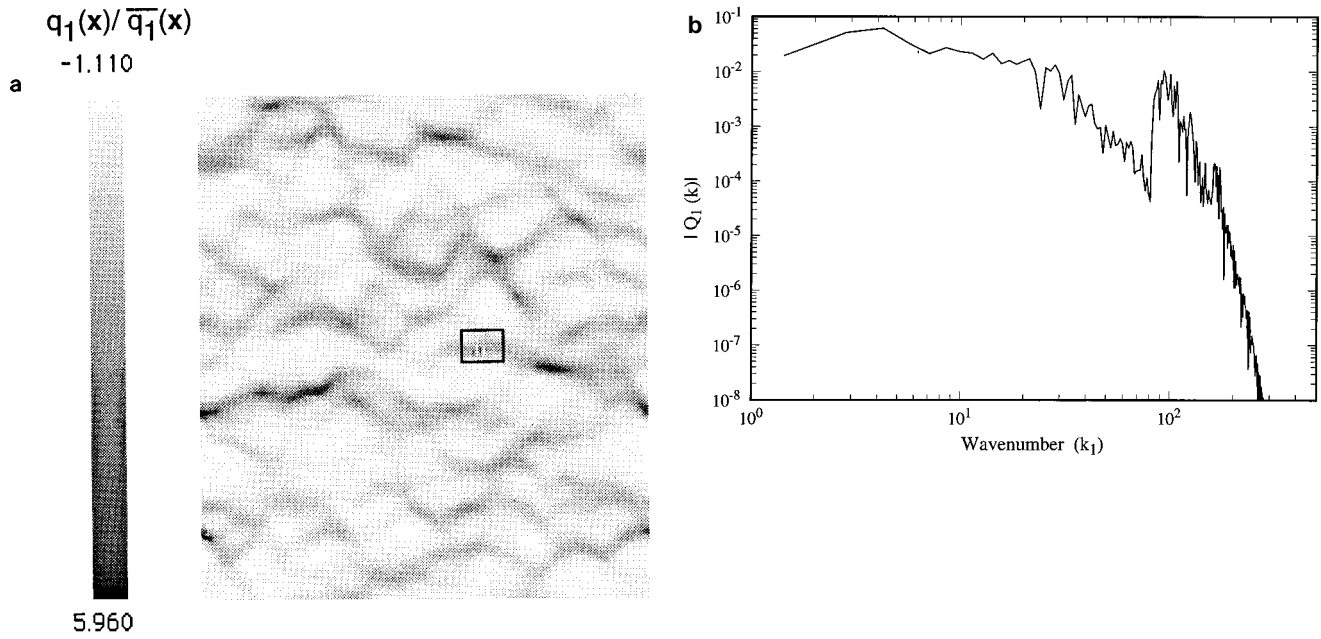


Figure 1. Errors in the specific discharge calculations appear in physical and wave spaces. (a) In physical space, local inaccuracies appear as Gibbs phenomena, shown here in the box. (b) In wave space, errors appear as aliasing errors at high wavenumbers.

memory and computational costs on the Cray Y-MP supercomputer. This discretization is generally more dense than the resolutions typically used for Monte Carlo simulations of flow. *Bellin et al.* [1992], for example, used 20,756 elements in the finite element solution. However, as discussed by *Beckie et al.* [1994], unresolved scales, or subgrid components, of velocity can interact with resolved scales in complex ways. We found that fine discretization was important for minimizing the importance of the subgrid components and subsequent interactions with the larger-scale components. As the log-conductivity variance increased, finer discretizations were required to resolve the specific discharge fluctuations. Typically, this required discretizations of 5–10 nodes per integral scale or finer. These discretizations effectively limited the range of log-

conductivity variances and correlation lengths that were feasible to investigate with a Monte Carlo approach.

The third procedure for minimizing error in estimating specific discharge variances is to take the numerical convergence criterion as zero divergence of the specific discharge. *Chin and Wang* [1992], *Bellin et al.* [1992], and *Bellin et al.* [1994] all note the importance of a convergence criterion that conserves mass. One can rewrite (9) in matrix form when the wavenumber domain is finite [*Van Lent*, 1992, p. 41] as

$$AH = b \quad (18)$$

where H is an $N \times 1$ vector, N is the total number of nodes, containing the Fourier coefficients of the head H , A is an $N \times N$ matrix, and b is an $N \times 1$ vector. This system is the matrix representation of (9) and, as such, is a reformulation of the continuity and Darcy's law applied to the fluctuating components. The solution to (18) is found through an iterative Richardson's procedure

$$H^{(i+1)} = H^{(i)} - \omega(AH^{(i)} - b) \quad (19)$$

where the superscript (i) refers to the iteration number. One can measure the Euclidean norm of the error and use it as the convergence criterion

$$\frac{\|AH^{(i)} - b\|}{\|b\|} < \varepsilon \quad (20)$$

where the norm is taken over all wavenumbers in the calculation. Typically, $\varepsilon < 10^{-5}$ was used as the convergence criterion. Simply using the relative change in the head fluctuations was inadequate to assure that continuity was satisfied everywhere in the domain. We found that convergence criteria of the form $\|H^{(i+1)} - H^{(i)}\|/\|H^{(i)}\|$ were unsatisfactory if accurate specific discharge calculations were required. Small errors in the small-scale head fluctuations (large wavenumber) components of

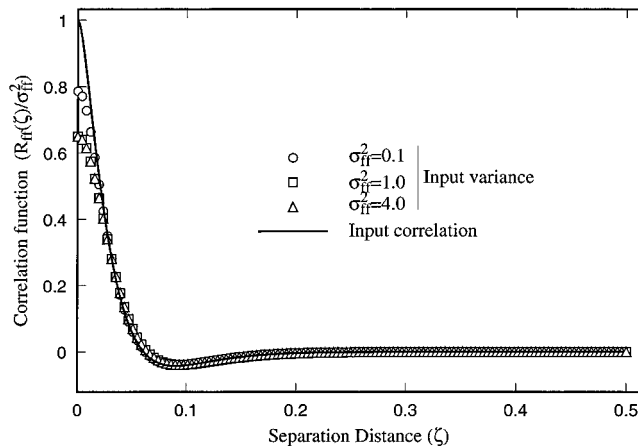


Figure 2. The effects of filtering the log-conductivity field on the log-conductivity covariance function. The input covariance is (23) with $\lambda = 0.02$. The log conductivity is filtered to disallow fluctuations at scales less than $1/85$ of the domain length.

$H(\mathbf{k})$ would often result in a corruption in the small-scale specific discharge fluctuations.

In summary, we applied a numerical spectral method that allowed an approximately stationary representation of log conductivity and head fluctuations. To assure a high degree of accuracy in the calculations and to avoid potential errors in the estimation of specific discharge moments, we placed restrictions on allowable log-conductivity scales, discretized the domain to at least 10 nodes per integral scale, and applied a strict convergence criterion based upon the conservation of mass. We then applied a Monte Carlo simulation procedure by generating random realization of the Fourier transform of log conductivity, calculated the resultant Fourier coefficients of head fluctuations and specific discharge fluctuations, and then estimated the resultant spectra via a method of moments approach.

Behavior of Head Fluctuations

In a small perturbation approximation the governing equation for flow is approximated by neglecting the product of fluctuating terms [Gelhar, 1993, p. 103]

$$(\partial^2 h / \partial x_i^2) \approx -J_i (\partial f / \partial x_i) \quad (21)$$

The above leads to a relation between the spectra of head and log conductivity

$$S_{hh}(\mathbf{k}) = \frac{(J_i k_i)^2}{4\pi^2 k^4} S_{ff}(\mathbf{k}) \quad (22)$$

with the head covariance then found by an inverse Fourier transform of the spectrum. Using (22) as the governing relation for flow, there are a number of analytical relationships available between log-conductivity covariance and head covariance. Mizell *et al.* [1982] used the log-conductivity covariance

$$R_{ff}(\xi) = \sigma_{ff}^2 \left[\left(\frac{\pi \xi}{4\lambda} \right) K_1 \left(\frac{\pi \xi}{4\lambda} \right) - \left(\frac{\pi \xi}{4\lambda} \right)^2 K_2 \left(\frac{\pi \xi}{4\lambda} \right) \right] \quad (23)$$

where $\xi^2 = \xi_i \xi_i$ and K_m is a modified Bessel function of order m . We used this log-conductivity covariance as a starting point because analytical small perturbation approximation relationships between log-conductivity covariance and the head covariance [Mizell *et al.*, 1982] and between log-conductivity covariance and specific discharge covariances [Graham and McLaughlin, 1989] are available. This log-conductivity covariance, combined with the small perturbation approximation in (21) and assuming that the direction of flow is oriented with the x_1 axis, will result in a spectrum of the head fluctuations given by

$$S_{hh}^{(a)}(\mathbf{k}) = J_1^2 \lambda^4 \sigma_{ff}^2 \left[\frac{\pi^3 k_1^2}{2k^2 \left[(2\pi\lambda k)^2 + \frac{\pi^2}{16} \right]^3} \right] \quad (24)$$

where the superscript (a) denotes the small perturbation approximation. Because the log-conductivity realizations were filtered and because of finite domain effects, (24) will not strictly hold. Rather, it is appropriate to compare Monte Carlo numerical results to numerical results obtained using the small perturbation methods; we applied the procedures described by Van Lent and Kitanidis [1989] to calculate the small perturbation approximations. In this way the effects of filtering the log conductivity and of approximating an infinite domain by a

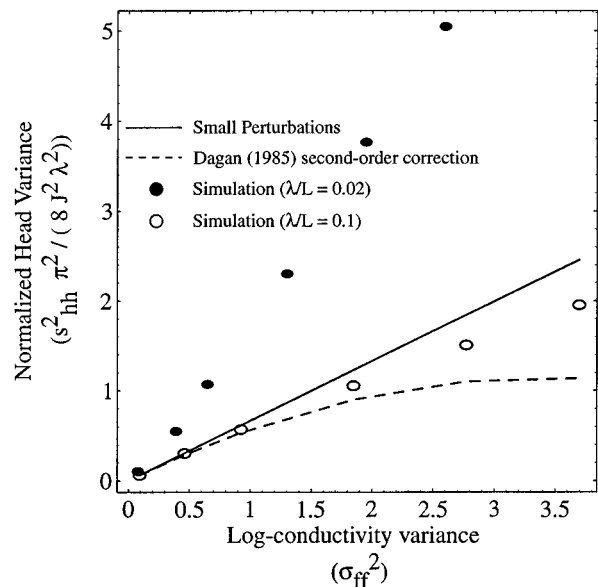


Figure 3. Comparison of calculated head variances versus prediction by the small perturbation approximation and by a second-order correction [Dagan, 1985].

finite domain do not cloud the interpretation since they are applied in the same fashion to both the Monte Carlo simulations and the small perturbation approximation.

One measure of variability is the total variance, which is the spectrum summed over all wavenumbers

$$\sigma^2 = \sum_{\text{all } \mathbf{k}} S(\mathbf{k}) \quad (25)$$

However, because we required that $h(\mathbf{x})$ be a zero-mean fluctuation, it must also be true that $H(\mathbf{0}) = 0$. In an infinite domain, $S(\mathbf{0})$ represents the variance at the infinite scale of fluctuation. In a finite domain, one can only estimate the scales of variability less than or equal to the domain size, so $S(\mathbf{0})$ cannot be directly estimated. It then becomes convenient to define a measure of the total variance in the finite domain as

$$s_{hh}^2 = \sum_{\substack{\text{all } \mathbf{k} \\ \mathbf{k} \neq \mathbf{0}}} S_{hh}(\mathbf{k}) \quad (26)$$

The above can then be used as a direct comparison between the analytical and numerical results for total variance, as it includes only variability at scales of interest.

One can begin to compare the effects of neglecting the nonlinear terms in (5) by looking at the head variances. Figure 3 compares the Monte Carlo simulation results at two different values of λ/L to the small perturbation approximation and the second-order correction of Dagan [1985]. Since all lengths are normalized to the domain size L , decreasing λ can be viewed as an increasing domain size relative to a fixed characteristic length parameter of the log conductivity. In Figure 3, one notes that the second-order correction improves the small perturbation estimate when the domain size is small but increasing domain size (decreasing λ) has the effect of significantly increasing the head variance. It would appear that the perturbation expansion of the governing equation (5) is not necessarily a convergent series. The importance of the scale interactions depends upon the scales of variability present, as well as the magnitude of the log-conductivity variance.

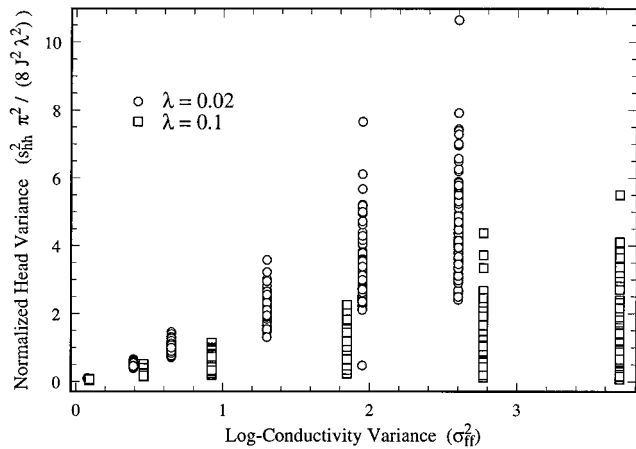


Figure 4. Calculated head variances for individual log-conductivity realizations. As the correlation length relative to the domain size decreases (increasing domain size), the variance in the head variance increases.

Another interesting feature of the head variance simulations is that the head fluctuations do not appear ergodic. Figure 4 shows the calculated head variances for two different values of λ in (23). As the domain size increases (decreasing λ), the variance of σ_{hh}^2 increases. In some investigations, such as *Ababou et al.* [1988, 1989], the spatial moments are used to approximate the ensemble moments, implicitly assuming ergodic behavior. Here we see that for the head fluctuations at least, increasing the domain size relative to the log-conductivity correlation length will not necessarily insure that ensemble moments will equal the spatial moments.

Figure 4 would also suggest that the small perturbation approximation tends to underpredict the head variances as the domain size becomes large. The source of the underprediction of variance and nonergodicity is most clearly seen by examination of the head spectrum. Figure 5 shows that the small wavenumber (large spatial scale) components of head variance are significantly larger than the small perturbation prediction. Moreover, these same small-wavenumber components increase with increasing log-conductivity contrast, which in turn

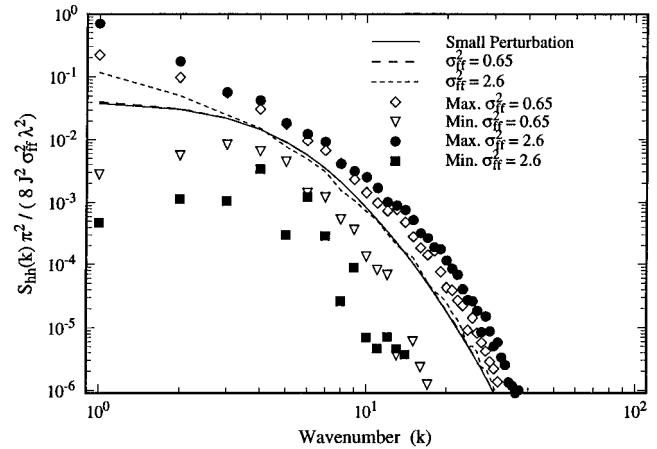
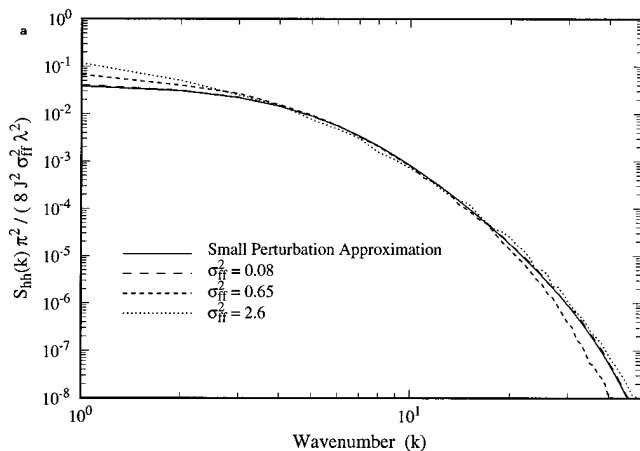


Figure 6. Range of estimates for the head spectrum, $S_{hh}(\mathbf{k})$, showing a cross section along the k_1 axis. As the log-conductivity variance increases, so does the range of the estimates for the large-scale components of head.

results in the apparent nonergodicity of head fluctuations. Another important difference between small perturbation approximation and the Monte Carlo simulations is the variability in the direction perpendicular to flow. As seen in (24) the small perturbation approximation neglects some of the variability of the head fluctuations transverse to the flow ($k_1 = 0$), but as the log-conductivity contrast grows, so does the head variability transverse to the flow. Again, one notes that the most significant variability is in the large-scale components and these components are underpredicted by the small perturbation approximation.

Figure 6 shows another aspect of the large-scale behavior of the head fluctuations. As the log-conductivity variance grows, the range of head variance which might be observed in any given realization increases with increased log-conductivity variability. This is particularly true at the largest scales. This would also suggest that most of the difference in head variance between realizations is due to large-scale fluctuations in head.

In terms of the variogram of head the effects of linearizing the governing equation show up in a number of ways. Figure 7

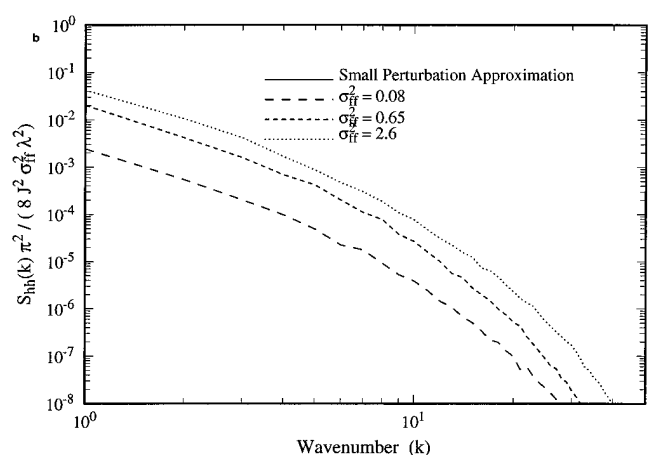


Figure 5. Spectrum of head fluctuations, $S_{hh}(\mathbf{k})$: (a) spectrum cross section along the k_1 axis and (b) spectrum cross section along the k_2 axis; the small perturbation approximation is exactly zero along the $k_2 = 0$ axis. The difference between the small perturbation approximation and the simulations is the growth of the large-scale components.

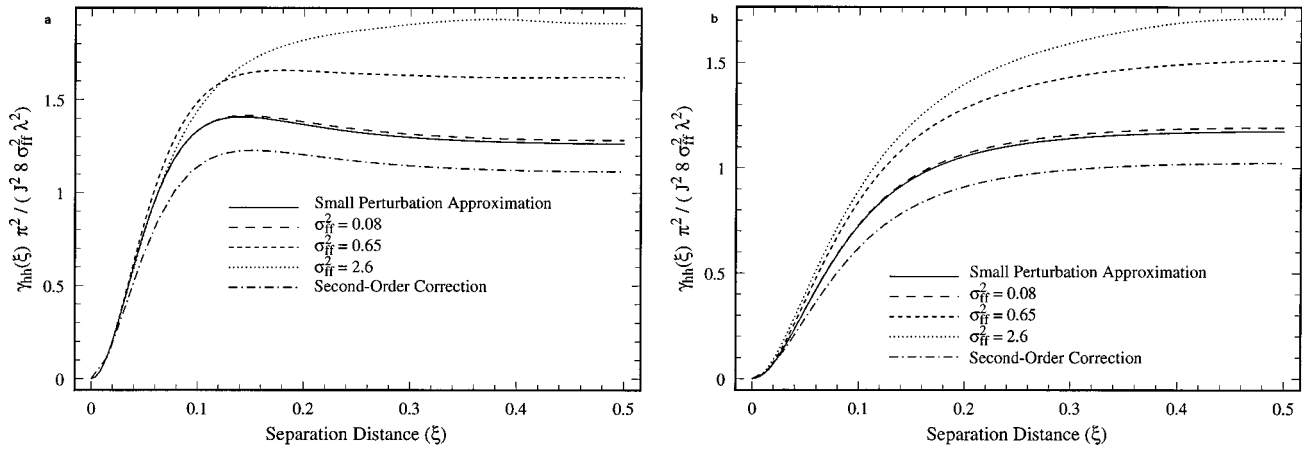


Figure 7. Variogram of head fluctuations, $\gamma_{hh}(\xi)$: (a) variogram cross section along the ξ_1 axis, in the direction of flow, and (b) variogram cross section along the ξ_2 axis, perpendicular to the direction of flow.

shows the effects of increased log-conductivity contrast on the head variogram for the case when $\lambda = 0.02$. In this case the estimates provided by Monte Carlo simulations tend to much higher sills, indicative of the higher overall total variance. At $\sigma_{ff}^2 = 2.60$ the small perturbation approximation underpredicts the total variance by 35%. The exact behavior of the far field depends upon the domain size, incorporated here into the λ parameter of the covariance; *Van Lent* [1992] provides other head variograms for different λ values and other log-conductivity generalized covariance functions. In all cases the variograms differ primarily in the far-field or large-scale components. As the domain size grows, so does the relative importance of the large-scale components and the more the small perturbation approximation underpredicts head variability.

Another interesting feature of the head variograms is that the hole effect, an artifact of requiring the head fluctuation to be finite in an infinite two-dimensional domain, quickly disappears as the log-conductivity variance grows. Even at moderate variances, $\sigma_{ff}^2 = 0.65$ in this case, the hole effect is substantially gone, with the result looking very similar to that for a Gaussian log-conductivity covariance function.

One can summarize the effects of the small perturbation approximation on the head fluctuations as follows. The effect of neglecting products of perturbations is not a uniform result

for all log-conductivity variances and domain sizes. Neglecting the products of perturbation results tends to underestimate the large-scale head fluctuations, and the underestimate grows with increasing domain size. Hence head fluctuations tend not to be ergodic. The relative importance of the large-scale head fluctuations also grows with log-conductivity variance, with significant differences between small perturbation and Monte Carlo estimates of variograms occurring well below σ_{ff}^2 of unity.

Specific Discharge Fluctuations

Dagan [1987] derived the small perturbation relation between the spectra of the log-conductivity and specific discharge components as

$$S_{q_{ff}}^{(a)}(\mathbf{k}) = K_G^2 \left(J_i - k_i \frac{k_i J_1}{k^2} \right) \left(J_j - k_j \frac{k_j J_1}{k^2} \right) S_{ff}(\mathbf{k}) \quad (27)$$

where the direction of flow is taken in the x_1 direction. *Graham and McLaughlin* [1989] applied the above relation to the covariance function (23) to derive a small perturbation approximation for the specific discharge covariance. Again, it is convenient to define a measure of the total specific discharge variance in a finite domain as

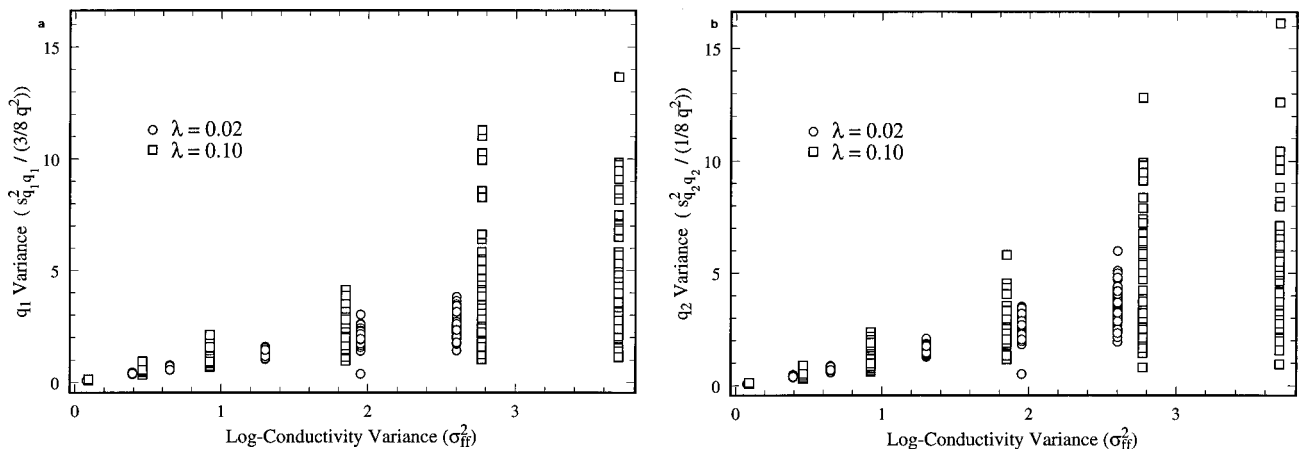


Figure 8. Total variance of specific discharge fluctuations: (a) variance of the q_1 component and (b) variance of the q_2 component.

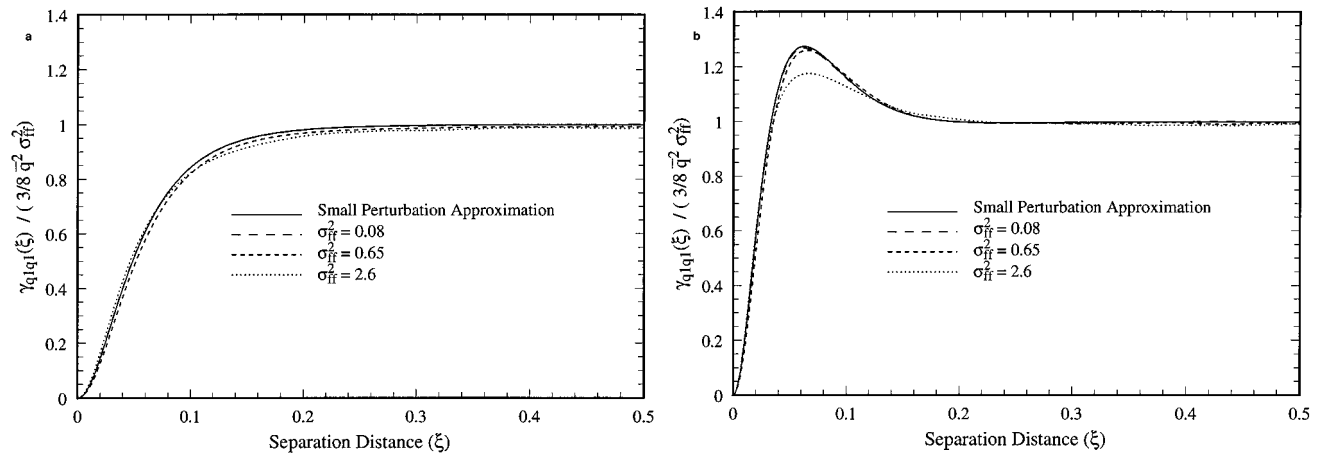


Figure 9. Comparison of the variogram of the specific discharge fluctuation in the direction of flow, $\gamma_{q_1 q_1}(\xi)$, to the small perturbation approximation: (a) cross section of $\gamma_{q_1 q_1}(\xi)$ in the ξ_1 direction and (b) cross section of $\gamma_{q_1 q_1}(\xi)$ in the ξ_2 direction.

$$s_{q_{ij}}^2 = \sum_{\substack{\text{all } \mathbf{k} \\ \mathbf{k} \neq 0}} S_{q_{ij}}(\mathbf{k}) \quad (28)$$

One singularly important characteristic of the specific discharge variances is that they appear ergodic, as shown in Figure 8. As the domain size increases, the variance of $s_{q_1}^2$ and $s_{q_2}^2$ decreases, in contrast to the head fluctuations. This is true for both the q_1 and the q_2 component. Apparently, taking the derivative of the head fluctuations was sufficient to dampen the large-scale effects contributing to the nonergodicity seen in the head. *Van Lent* [1992, p. 256] also demonstrates that a Gaussian log-conductivity covariance will also yield similar behavior.

The variogram of the longitudinal component of specific discharge q_1 is very similar to the small perturbation approximation. Figure 9 compares the small perturbation approximation to Monte Carlo solutions, and the results are nearly identical. We found that the variogram of the longitudinal component of specific discharge closely matched the small perturbation approximation in nearly all respects for all values of log-conductivity contrast ($0.1 \leq \sigma_{ff}^2 \leq 3.4$) and log-conductivity covariance functions that we examined [*Van Lent*, 1992]. It would appear that the small perturbation approxima-

tion is a robust estimator of the generalized covariance of the longitudinal component of specific discharge.

The transverse component of specific discharge q_2 shows some significant differences between the linearized approximation and the Monte Carlo simulations, however. Figure 10 contrasts the variogram for the case where (23) is used as log-conductivity covariance with $\lambda = 0.02$. The Monte Carlo simulations show much higher total variances. A more qualitative comparison is seen in Figure 11. The small perturbation approximation displays strong correlations along transects that are at 45° angles from the axis of flow, while the Monte Carlo simulations show correlations in those directions but much weaker than predicted by the small perturbation approximation. Overall, the transverse component of specific discharge shows much less coherence and much higher variance than predicted by the small perturbation approximation.

Cross sections of the $S_{q_1 q_1}(\mathbf{k})$ and $S_{q_2 q_2}(\mathbf{k})$ (Figures 12–13) spectra illustrate that as in the case of head fluctuations, the important differences between the Monte Carlo simulations and the small perturbation approximation occur in the large-scale components. This is especially true of the cross section in

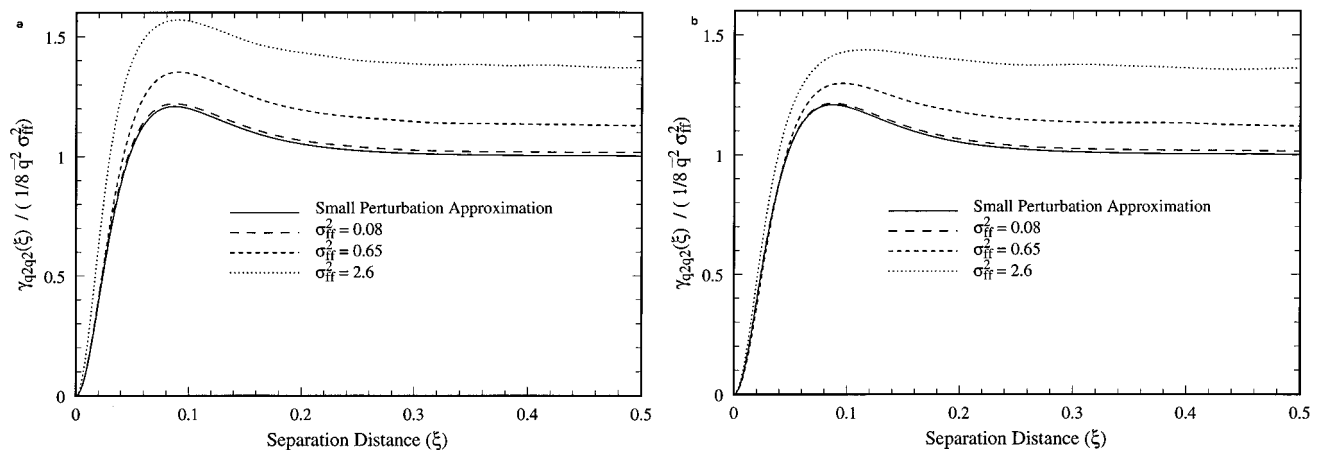


Figure 10. Comparison of the variogram of the specific discharge fluctuation perpendicular to the direction of flow, $\gamma_{q_2 q_2}(\xi)$, to the small perturbation approximation: (a) cross section of $\gamma_{q_2 q_2}(\xi)$ in the ξ_1 direction and (b) cross section of $\gamma_{q_2 q_2}(\xi)$ in the ξ_2 direction.

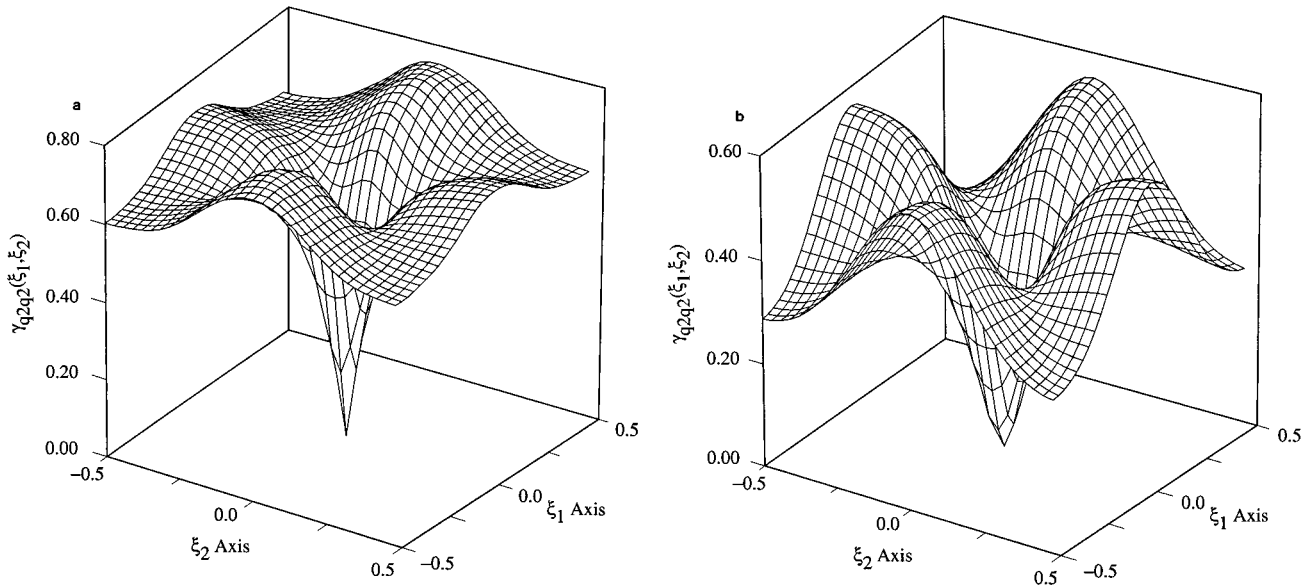


Figure 11. A qualitative comparison of the variogram of the specific discharge fluctuation perpendicular to the direction of flow, $\gamma_{q_2 q_2}(\xi)$, to the small perturbation approximation ($\sigma_{ff}^2 = 3.6$, $\lambda = 0.1$): (a) estimate from Monte Carlo simulations and (b) small perturbation approximation.

along the k_2 axis. The small perturbation approximation neglects the contributions along this axis, yet the Monte Carlo simulations show that even at log-conductivity variances less than unity, these components are the same order of magnitude as the dominant components in the small perturbation approximation. In general, the small perturbation approximation underpredicts the large-scale variability in q_2 as log conductivity becomes large, primarily by underpredicting the fluctuations in q_2 transverse to the direction of flow.

Conclusions

Numerical spectral methods are the analog to analytical approaches and are useful in assessing the effects of neglecting scale interactions resulting from first-order approximations to the governing equations for groundwater flow. The Fourier methods used in this spectral approach can approximate sta-

tionarity in a finite domain to an arbitrary degree. When accurate calculations of specific discharge are required, strict adherence to continuity is essential. In a spectral approach this was accomplished by filtering the log-conductivity fluctuations, using a fine discretization, and applying a strict convergence criterion based upon continuity.

In comparing the results of Monte Carlo simulations to the small perturbation approximation for head and specific discharge, we found that the effects of neglecting the scale interactions depend upon the domain size as well as the log-conductivity variance. As the domain size increases, the effects of large-scale head fluctuations predominate, and these large-scale head fluctuations tend to be underestimated by a first-order approximation as well as the second-order corrections. Also, the head fluctuations have a nonergodic behavior; as the domain size grows, the variance of σ_{hh}^2 tends to increase.

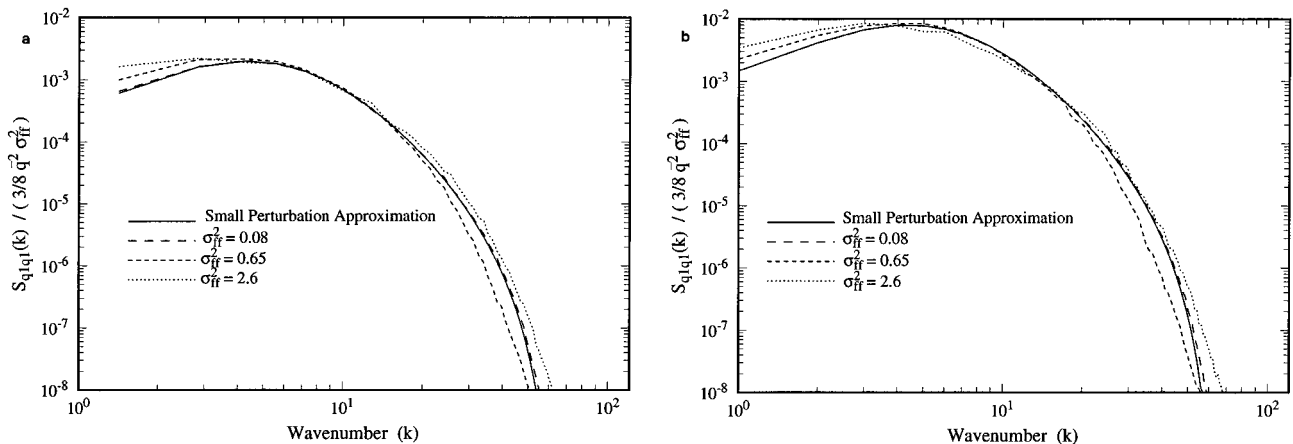


Figure 12. Comparison of the spectrum of the specific discharge component in the direction of flow, $S_{q_1 q_1}(\mathbf{k})$, to the small perturbation approximation: (a) cross section of $S_{q_1 q_1}(\mathbf{k})$ where $k_1 = k_2$ and (b) cross section of $S_{q_1 q_1}(\mathbf{k})$ along the k_2 axis.

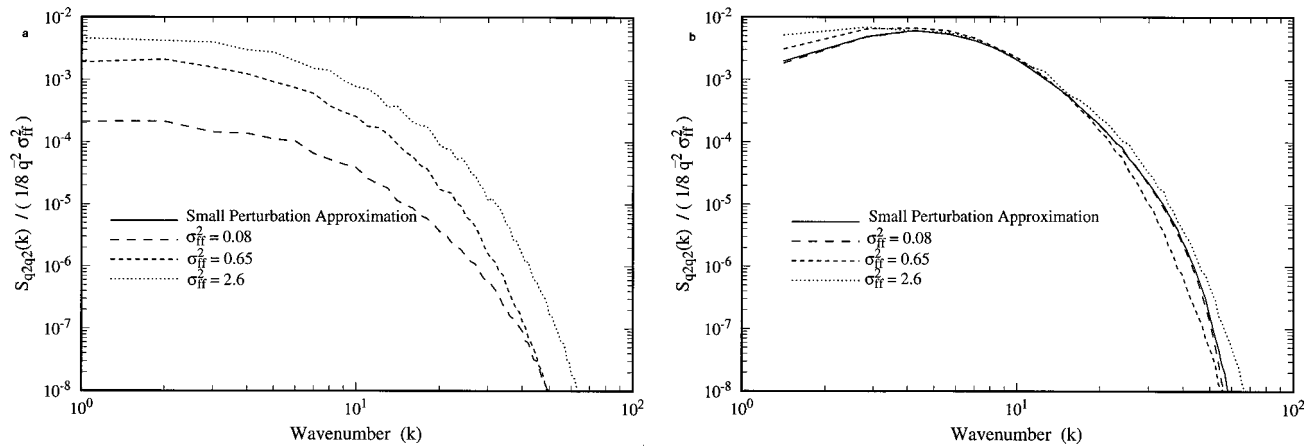


Figure 13. Comparison of the spectrum of the specific discharge component perpendicular to the direction of flow, $S_{q_2 q_2}(\mathbf{k})$, to the small perturbation approximation: (a) cross section of $S_{q_2 q_2}(\mathbf{k})$ where $k_1 = k_2$ and (b) cross section of $S_{q_2 q_2}(\mathbf{k})$ along the k_2 axis; the small perturbation approximation is exactly zero along this axis.

The specific discharge fluctuations in both the longitudinal and the transverse directions display a clearly ergodic behavior. Moreover, the small perturbation approximation is a very robust predictor of the covariance of the longitudinal component of the specific discharge vector. This was true for log-conductivity variances past 3.0, as well as various log-conductivity covariance functions. The small perturbation approximation underpredicted the total variance of the transverse component of specific discharge, however. The large-scale components of the transverse component of specific discharge were underpredicted by the small perturbation approximation. This was particularly true for the large-scale components of variability transverse to the direction of flow.

Acknowledgments. Work was supported by the National Science Foundation under grants EET-876585 and BCS-8914812, the U.S. Geological Survey Water Resources Research Grant Program under grant 14-08-001-G1491, and the Office of Research and Development, U.S. EPA, under agreement R-815738-01 through the Western Region Hazardous Substance Center. Computation facilities were made possible by a grant from the San Diego Supercomputer Center. The content of this study does not necessarily represent the views of these agencies. The authors would like to thank Alberto Bellin, David Chin, and Vivek Kapoor for their insightful and helpful comments.

References

- Ababou, R., L. W. Gelhar, and D. McLaughlin, Three dimensional flow in random porous media, *Tech. Rep. 318*, Ralph M. Parsons Lab., Mass. Inst. of Technol., Cambridge, Mass., 1988.
- Ababou, R., D. McLaughlin, and A. Tompson, Numerical simulation of three-dimensional saturated flow in randomly heterogeneous porous media, *Trans. Porous Media*, 4, 549–565, 1989.
- Bakr, A. A., L. W. Gelhar, A. L. Gutjahr, and J. R. MacMillan, Stochastic analysis of spatial variability in subsurface flows, 1, Comparison of one- and three-dimensional flows, *Water Resour. Res.*, 14(2), 263–271, 1978.
- Beckie, R., A. Aldama, and E. Wood, The universal structure of the groundwater flow equations, *Water Resour. Res.*, 30(5), 1407–1419, 1994.
- Bellin, A., P. Salandin, and A. Rinaldo, Simulation of dispersion in heterogeneous porous formations: Statistics, first-order theories, convergence of computations, *Water Resour. Res.*, 28(9), 2211–2277, 1992.
- Bellin, A., Y. Rubin, and A. Rinaldo, Eulerian-Lagrangian approach for modeling flow and transport in heterogeneous geological formations, *Water Resour. Res.*, 30(11), 2913–2924, 1994.
- Chin, D., and T. Wang, An investigation of the validity of first-order stochastic dispersion theories in isotropic porous media, *Water Resour. Res.*, 28(6), 1531–1542, 1992.
- Dagan, G., Stochastic modeling of groundwater flow by unconditional and conditional properties, 1, Conditional simulation and the direct problem, *Water Resour. Res.*, 18(4), 813–833, 1982a.
- Dagan, G., Analysis of flow through heterogeneous random aquifers, 2, Unsteady flow in confined aquifers, *Water Resour. Res.*, 18(5), 1571–1585, 1982b.
- Dagan, G., A note on higher-order corrections of the head covariances in steady aquifer flow, *Water Resour. Res.*, 21(4), 573–578, 1985.
- Dagan, G., Theory of solute transport by groundwater, *Annu. Rev. Fluid Mech.*, 19, 183–215, 1987.
- Dagan, G., Time-dependent macrodispersion for solute transport in anisotropic heterogeneous aquifers, *Water Resour. Res.*, 24(9), 1491–1500, 1988.
- Dagan, G., *Flow and Transport in Porous Formations*, 465 pp., Springer-Verlag, New York, 1989.
- Dagan, G., and S. Neuman, Nonasymptotic behavior of a common Eulerian approximation for transport in random velocity fields, *Water Resour. Res.*, 27(12), 3249–3256, 1991.
- Dettinger, M., and J. L. Wilson, First order analysis of uncertainty in numerical models of groundwater flow, 1, Mathematical development, *Water Resour. Res.*, 17(1), 149–161, 1981.
- Dikow, E., Stochastic analysis of groundwater flow in a bounded domain by spectral methods, *Trans. Porous Media*, 3, 173–184, 1988.
- Dykaar, B., and P. K. Kitanidis, Determination of effective hydraulic conductivity for heterogeneous porous media using a numerical spectral approach, 1, Method, *Water Resour. Res.*, 28(4), 1155–1166, 1992.
- Fiorotto, V., and A. Giorgini, Stochastic analysis of groundwater flow by spectral analysis, in *Proceedings of the Sixth IAHR International Symposium on Stochastic Hydrology*, edited by J. Kuo and G. Lin, pp. 517–524, Water Resour. Publ., Fort Collins, Colo., 1992.
- Gelhar, L. W., Effects of hydraulic conductivity variations on groundwater flow, in *Hydraulic Problems Solved by Stochastic Methods*, edited by P. Hjorth, L. Jönsson, and P. Larson, pp. 409–431, Water Resour. Publ., Fort Collins, Colo., 1977.
- Gelhar, L. W., *Stochastic Subsurface Hydrology*, 390 pp., Prentice-Hall, Englewood Cliffs, N. J., 1993.
- Gelhar, L. W., and C. L. Axness, Three-dimensional stochastic analysis of macrodispersion in aquifers, *Water Resour. Res.*, 19(1), 161–180, 1983.
- Graham, W., and D. McLaughlin, Stochastic analysis of nonstationary solute transport, 1, Unconditional moments, *Water Resour. Res.*, 25(2), 215–232, 1989.
- Gutjahr, A., Fast Fourier transform for random field generation, tech-

- nical report project report, contract 4-RS of Los Alamos National Laboratory, N. M. Inst. of Min. and Technol., Socorro, N. M., 1989.
- Gutjahr, A., L. W. Gelhar, A. A. Bakr, and J. R. MacMillan, Stochastic analysis of spatial variability in subsurface flows, 2, Estimation and application, *Water Resour. Res.*, 14(5), 953–959, 1978.
- Jones, L., Some results comparing Monte Carlo simulations and first order Taylor series approximations for steady groundwater flow, *Stochastic Hydrol. Hydraul.*, 3(3), 179–190, 1989.
- Li, S.-H., and D. McLaughlin, A nonstationary spectral method for solving stochastic groundwater problems: Unconditional analysis, *Water Resour. Res.*, 27(7), 1589–1605, 1991.
- Li, S.-H., and D. McLaughlin, Using the nonstationary spectral method to analyze flow through heterogeneous trending media, *Water Resour. Res.*, 31(3), 541–552, 1995.
- Mizell, S. A., A. L. Gutjahr, and L. W. Gelhar, Stochastic analysis of spatial variability in two-dimensional steady groundwater flow assuming stationary and nonstationary fields, *Water Resour. Res.*, 18(4), 1053–1067, 1982.
- Neuman, S. P., C. L. Winter, and C. M. Newman, Stochastic theory of field-scale Fickian dispersion in anisotropic porous media, *Water Resour. Res.*, 23(3), 453–466, 1987.
- Priestley, M. B., *Spectral Analysis and Time Series*, 890 pp., Academic, San Diego, Calif., 1981.
- Robin, M., A. Gutjahr, E. Sudicky, and J. Wilson, Cross-correlated random field generation with the direct Fourier transform method, *Water Resour. Res.*, 29(7), 2385–2397, 1993.
- Rubin, Y., Stochastic modeling of macrodispersion in heterogeneous porous media, *Water Resour. Res.*, 26(1), 133–141, 1990.
- Rubin, Y., and G. Dagan, Stochastic analysis of boundaries effects on head spatial variability in heterogeneous aquifers, 1, Constant head boundary, *Water Resour. Res.*, 24(10), 1689–1697, 1988.
- Rubin, Y., and G. Dagan, Stochastic analysis of boundaries effects on head spatial variability in heterogeneous aquifers, 2, Impervious boundary, *Water Resour. Res.*, 25(4), 707–712, 1989.
- Sagar, B., Galerkin finite element procedure for analyzing flow through random media, *Water Resour. Res.*, 14(6), 1035–1044, 1978.
- Smith, L., and R. A. Freeze, Stochastic analysis of steady state groundwater flow in a bounded domain, 1, One-dimensional simulations, *Water Resour. Res.*, 15(3), 521–528, 1979a.
- Smith, L., and R. A. Freeze, Stochastic analysis of steady state groundwater flow in a bounded domain, 2, Two-dimensional simulations, *Water Resour. Res.*, 15(6), 1543–1559, 1979b.
- Smith, L., and F. W. Schwartz, Mass transport, 1, A stochastic analysis of macroscopic dispersion, *Water Resour. Res.*, 16(2), 303–313, 1980.
- Smith, L., and F. W. Schwartz, Mass transport, 2, Analysis of uncertainty in prediction, *Water Resour. Res.*, 17(2), 352–369, 1981.
- Van Lent, T., Numerical spectral methods applied to flow in highly heterogeneous aquifers, Ph.D. thesis, Stanford Univ., Stanford, Calif., 1992.
- Van Lent, T., and P. K. Kitanidis, A numerical spectral approach for the derivation of piezometric head covariance functions, *Water Resour. Res.*, 25(11), 2287–2298, 1989.

P. K. Kitanidis, Department of Civil Engineering, Stanford University, Stanford, CA 94305. (e-mail: pkk@ce.stanford.edu)

T. Van Lent, Department of Civil and Environmental Engineering, South Dakota State University, Box 2219, Brookling, SD 57007. (e-mail: vanlent@anpawhi.sdstate.edu)

(Received July 10, 1995; revised January 5, 1996; accepted January 13, 1996.)